Neurobiology of Disease **8,** 847–865 (2001)
doi:10.1006/nbdi.2001.0428, *available online at http://www.idealibrary.com on* IDEAL®

Gene Expression Profiling in Postmortem Rett Syndrome Brain: Differential Gene Expression and Patient Classification

Carlo Colantuoni,*,† Ok-Hee Jeon,*,† Karim Hyder,‡ Alex Chenchik,‡ Anis H. Khimani,§,1 Vinodh Narayanan,¶ Eric P. Hoffman,‖ Walter E. Kaufmann,**,††,‡‡ SakkuBai Naidu,‡‡,§§ and Jonathan Pevsner*,†

**Department of Neurology, **Department of Cognitive Neurology, and §§Department of Neurogenetics, Kennedy Krieger Institute, 707 North Broadway, Baltimore, Maryland 21205; †Department of Neuroscience, ‡‡Departments of Neurology and Pediatrics, Johns Hopkins University School of Medicine, 725 North Wolfe Street, Baltimore, Maryland 21205; ‡CLONTECH Laboratories, Inc., Palo Alto, California 94303; §Perkin–Elmer NEN Life Science, Inc., Boston, Massachusetts 02118; ¶Department of Neurology, Children's Hospital of Pittsburgh, Pittsburgh, Pennsylvania 15213; ‖Research Center for Genetic Medicine, Children's National Medical Center, Washington, D.C.; and ††Departments of Pathology and Psychiatry and Behavirol Science, Johns Hopkins Hospital, Baltimore, Maryland 21205.*

Received May 9, 2001; revised June 14, 2001; accepted June 22, 2001

The identification of mutations in the transcriptional repressor methyl-CpG-binding protein 2 (*MECP2*) gene in Rett Syndrome (RTT) suggests that an inappropriate release of transcriptional silencing may give rise to RTT neuropathology. Despite this progress, the molecular basis of RTT neuropathogenesis remains unclear. Using multiple cDNA microarray technologies, subtractive hybridization, and conventional biochemistry, we generated comprehensive gene expression profiles of postmortem brain tissue from RTT patients and matched controls. Many glial transcripts involved in known neuropathological mechanisms were found to have increased expression in RTT brain, while decreases were observed in the expression of multiple neuron-specific mRNAs. Dramatic and consistent decreases in transcripts encoding presynaptic markers indicated a specific deficit in presynaptic development. Employing multiple clustering algorithms, it was possible to accurately segregate RTT from control brain tissue samples based solely on gene expression profile. Although previously achieved in cancers, our results constitute the first report of human disease classification using gene expression profiling in a complex tissue source such as brain.

INTRODUCTION

Rett Syndrome (OMIM No. 312750: RTT) is a developmental neurological syndrome that occurs almost exclusively in females (Hagberg *et al.*, 1983; Armstrong, 1997; Naidu, 1997). Affected females are apparently normal through pre- and perinatal development, following which there is a developmental arrest. This is accompanied by decelerated head and brain growth, loss of speech and social skills, severe mental retardation, truncal ataxia, and characteristic hand-wringing motions. Prominent neuropathological features include reductions in cortical thickness in multiple cerebral cortical regions, decreased neuronal soma size, reduced number of identifiable synapses, and dramatically decreased dendritic arborization with increased neuronal cell packing density, but without a gross reduction in neuronal cell numbers (Jellinger *et al.*, 1988; Belichenko *et al.*, 1994; Bauman *et al.*, 1995a,b; Belichenko *et al.*, 1997; Kaufmann *et al.*, 1997).

[1] Current address: Corning Microarray Technologies, Corning, New York 14831.

0969-9961/01 $35.00

Mutations in the coding region of the X-linked methyl-CpG-binding protein 2 (*MECP2*) gene have been identified in 60–80% of clinically defined RTT cases (Amir *et al.*, 1999; Wan *et al.*, 1999; Amano *et al.*, 2000; Bienvenu *et al.*, 2000; Buysc *et al.*, 2000; Cheadle *et al.*, 2000; De Bona *et al.*, 2000; Hampson *et al.*, 2000; Huppke *et al.*, 2000; Kim and Cook, 2000; Obata *et al.*, 2000; Xiang *et al.*, 2000; Nielsen *et al.*, 2001; Vacca *et al.*, 2001). MeCP2 binds to methylated CpG dinucleotides and is involved in methylation-dependent repression of gene expression via the recruitment of corepressors, including mSin3A and the chromatin remodeling histone deacetylases HDAC1 and HDAC2 (Nan *et al.*, 1998a,1998b; Ng and Bird, 1999). The expression of MeCP2 mRNA in many tissues and its interaction with regulatory DNA elements in multiple chromosomes suggest that MeCP2 is a global repressor of gene expression (Nan *et al.*, 1997). DNA methylation-dependent repression of gene expression has been associated with genetic imprinting, X chromosome inactivation, carcinogenesis, and tissue-specific gene expression (Cedar, 1988; Allaman-Pillet *et al.*, 1998; Constancia *et al.*, 1998; Razin, 1998; Cameron *et al.*, 1999; Ng and Bird, 1999).

The large number of distinct mutations in the *MECP2* gene that have been associated with RTT strongly suggests that RTT is the result of a loss of MeCP2 function. However, several other findings indicate that the identified mutations do not all simply lead to a complete loss of function (Amir *et al.*, 2000; Amir and Zoghbi, 2000; Dragich *et al.*, 2000; Van den Veyver and Zoghbi, 2000; Nielsen *et al.*, 2001; Shahbazian and Zoghbi, 2001). Several mutations in the *MECP2* gene have been determined to cause neurological phenotypes distinct from RTT (Couvert *et al.*, 2001; Watson *et al.*, 2001). In addition, a number of *MECP2* mutations have been identified in males displaying a range of neurological phenotypes (Clayton-Smith *et al.*, 2000; Meloni *et al.*, 2000; Orrico *et al.*, 2000; Imessaoudene *et al.*, 2001; Watson *et al.*, 2001). If the *MECP2* mutations identified in RTT represent a heterogeneous spectrum of distinct loss-of-function mutations, these mutations might be expected to have a global impact on gene expression through a release of transcriptional silencing.

Although MeCP2 mRNA is expressed in cells throughout the body, *MECP2* mutations in RTT lead to a primarily neurological phenotype. For this reason we have selected brain tissue to begin the investigation of gene expression changes in RTT. We have characterized mRNA expression in postmortem brain tissue from six RTT patients and six matched control subjects. In order to generate comprehensive gene expression profiles we have used four independent cDNA microarray technologies in addition to subtractive cDNA hybridization techniques and RT-PCR. Using these techniques, we have identified a large number of genes whose expression is consistently differentially regulated in RTT. In addition, clustering algorithms were successfully employed to distinguish RTT from control brain tissue samples based only on gene expression information derived from the microarray analysis.

METHODS

Sample Acquisition

We obtained 0.5 to 1 g of cerebral cortex from 6 female RTT brains and 6 age- and gender-matched controls. Tissue was dissected by a pediatric neuropathologist (W.E.K.) from the junction of frontal and parietal cortices corresponding to Brodmann's areas 1–5. Clinical details for RTT cases and controls are in Table 1. At varying times prior to death, the majority of these RTT patients received medications including benzodiazapines and antiepileptic drugs.

Methods used in the dissection of brain tissue were identical in all cases. Identical regions were dissected from all disease-control matched brains and care was taken to dissect primarily gray matter in all cases. Depending on amount of tissue available, more or less tissue was dissected from any one brain sample, resulting in a range of different values for the total amount of tissue dissected.

Total RNA was purified using TRIzol (GIBCO/BRL). For CLONTECH arrays RNA was additionally extracted with phenol-chloroform and mRNA was isolated with poly-d(T) magnetic beads (Boehringer Mannheim). mRNA isolation for UniGEM V arrays was performed with RNeasy mRNA isolation kits (Qiagen) following TRIzol extraction. RNA purity was confirmed by monitoring the ratio of absorbance (A260/A280) in a spectrophotometer (Spectronic GeneSys 5). Integrity of RNA samples (absence of degradation of ribosomal RNAs) was confirmed by electrophoresis of the RNA on agarose gels (data not shown). The integrity of the RNA was adequate to reliably allow reverse transcription of specific cDNAs. For immunoblotting and genomic DNA sequencing experiments, protein and DNA were extracted from remaining TRIzol phases according to the manufacturer's protocol.

TABLE 1
Clinical Information on Brain Specimens Used

Case	Diagnosis	Sex	Age	PMI	Cause of death	Brain region
R1	RTT	F	2	20	RTT complications in sleep	Brodmann's 1–5
R2	RTT	F	10	5	Prolonged fever, cardiac arrest	Brodmann's 1–5
R3	RTT	F	25	11	Heart attack	Brodmann's 1–5
R4	RTT	F	29	35	Seizures; respiratory obstruction	Brodmann's 1–5
R5	RTT	F	19	<24	Heart attack	Brodmann's 1–5
R6	RTT	F	19	15	Seizure—died in sleep	Brodmann's 1–5
C1	Control	F	2	11	Meningitis—fever, seizures	Brodmann's 1–5
C2	Control	F	5	36	Cardiac arrhythmia	Brodmann's 1–5
C3	Control, MR	F	15	16	Bowel disease	Brodmann's 1–5
C4	Control	F	18	29	Accident; multiple injuries	Brodmann's 1–5
C5	Control	F	19	17	Accident; multiple injuries	Brodmann's 1–5
C6	Control	F	18	16	Accident; multiple injuries	Brodmann's 1–5

Note. Explanations and abbreviations: F, female; Age, age in years at time of death; PMI, postmortem interval in hours; MR, mental retardation.

Genomic DNA Sequencing

Genomic DNA corresponding to the entire coding region of MeCP2 was sequenced from 6 RTT brains. Oligonucleotide primers were used to amplify 10 distinct portions of the *MECP2* gene by PCR for sequencing. For all but one of these 10 PCR products, nested PCR primers were used to ensure specificity. The forward (F) and reverse (R) oligonucleotide primer pairs for exon 1 were the following: (F) 5′-TGTGTTTATCTTCAAAATG-3′ and (R) 5′-GTTATGTCTTTAGTCTTTGG-3′ with nested primers (F) 5′-GCAGCTCAATGGGGGCTTTC-3′ and (R) 5′-AGATGGCCAAACCAGGACAT-3′. For exon 2, the first primer pairs used were (F) 5′-AGCCCGTGCAGCCATCAGCC-3′ and (R) 5′-CCTGCACAGATCGGATAGAAG-3′ with nested primers (F) 5′-AGCCCGTGCAGCCATCAGCC-3′ and (R) 5′-CCCTGGGCACATACATTTTC-3′. A second fragment of exon 2 was amplified with primers (F) 5′-CTGCAGACTGGCATGTTCTC-3′ and (R) 5′-GGGGTCATCATACATGGGTCC-3′ without any nested primers. Exon 3 was sequenced in seven fragments. Two were derived from the primer pairs (F) 5′-AGCCCGTGCAGCCATCAGCC-3′ and (R) 5′-CCTGCACAGATCGGATAGAAG-3′ with the two pairs of nested primers (F) 5′-TTTGTCAGAGCGTTGTCACC-3′ and (R) 5′-CTTCCCAGGACTTTTCTCCA-3′; and then (F) 5′-AACCACCTAAGAAGCCCAAA-3′ and (R) 5′-CCTGCACAGATCGGATAGAAG-3′. The remaining five fragments of exon 3 were amplified using primers (F) 5′-GGCAGGAAGCGAAAAGCTGA-3′ and (R) 5′-GCTTTGTCAGAGCCCTACCC-3′ with the five nested primer pairs (F) 5′-GGCAGGAAGCGAAAAGCTGA-3′ and (R) 5′-CTCCCTCCCCTCGGTGTTTG-3′; (F) 5′-TGAGCCCGAGAGCTCCGAGG-3′ and (R) 5′-GGTTTGCTTTGCAATCCGCTC-3′; (F) 5′-GGAGAAGATGCCCAGAGGAG-3′ and (R) 5′-GCTTTGTCAGAGCCCTACCC-3′; (F) 5′-TGGTGAAGCCCCTGCTGGT-3′ and (R) 5′-CTCCCTCCCCTCGGTGTTTG-3′; (F) 5′-GGCAGGAAGCGAAAAGCTGA-3′ and (R) 5′-TGAGTGGTGGTGATGGTGGTGG-3′. To confirm detected mutations, each mutation was observed in at least four independent PCR reactions from genomic DNA. Sequencing was performed on both strands.

cDNA Sequencing

Mutations found in genomic DNA were further confirmed by sequencing cDNA derived from poly-d(T) primed reverse transcription of RNA extracted from postmortem brain samples. Sequence from only one strand was used for this confirmation. cDNA samples were PCR amplified for sequencing using the following primers: For subject R1 (F) 5′-CTGCCTGAAGGCTGGACACGG-3′ and (R) 5′-CTTCCCAGGACTTTTCTCCA-3′; for subjects R3 and R5 (F) 5′-GGCAGGAAGCGAAAAGCTGA-3′ and (R) 5′-CCTCGGAGCTCTCGGGCTCA-3′.

X Inactivation Studies

Genomic DNA isolated from the cerebellum was used to determine the X chromosome inactivation patterns in RTT patients R1–R6. A polymorphic CAG

repeat in the 5′ coding region of the human androgen receptor was used to differentiate the two X chromosomes in each individual. The PCR primers used to amplify this repeat are described elsewhere (Pegoraro *et al.*, 1994). This trinucleotide repeat is consistently methylated on the inactive X chromosome and unmethylated on the active X chromosome. Using the *Cfo*I and *Hpa*II methylation-sensitive enzymes (Boehringer-Mannheim) prior to PCR amplification, the unmethylated (active) allele is digested and hence not amplified. Quantification and comparison of PCR products obtained from digested and undigested genomic DNA samples yields a measure of percent of total activity for each allele; and hence for each X chromosome. This figure was determined by replicate trials.

Microarray Data Acquisition and Analysis

mRNA extracted from postmortem brains R1–R4 and C1–C4 was reverse transcribed with 597 gene-specific primers to generate radiolabeled cDNA probes for use with the Human Atlas and Human Atlas Neurobiology microarrays (CLONTECH Laboratories, Inc.; www.clontech.com). Each of these arrays consists of 597 cDNAs spotted in duplicate onto nylon filters. Radiolabeled probes were individually hybridized to arrays, washed, and levels of expressed genes were quantified by phosphorimaging. Using the MICOMAX microarray system (NEN Life Science Products, Inc.; www.nen.com) total RNA samples (4 μg) from cases R2–R4 and C2–C4 were also reverse transcribed to generate haptenated probes, hybridized to MICROMAX arrays, and detected by Tyramide Signal Amplification (TSA) using Cyanine 5 Tyramide deposition (for each RTT case) or Cyanine 3 Tyramide deposition (for each control case). These microarrays on glass slides consist of PCR products derived from inserts in bacterial plasmids corresponding to 2400 characterized mRNA sequences. Pairwise comparisons were made for C2 and R2, C3 and R3, and C4 and R4.

mRNA derived from an independent sampling of postmortem tissue was used to generate fluorescently labeled probes for use with Incyte Genomics UniGEM V 1.0 microarrays (www.incyte.com) representing 7075 human genes. Poly(A) + RNA (600 ng) was reverse transcribed to generate cDNA probes labeled with Cyanine 5 (for cases R2–R6) or Cyanine 3 (for a pool of control cases C1–C6). Each of these five individual RTT samples R2–R6 was hybridized simultaneously with the control pool to five UniGEM V microarrays at GenomeSystems.

Quantification of expression data from all array technologies included the subtraction of background signal followed by global normalization, i.e., all individual gene expression values were normalized to the global mean of all arrayed elements for that single array experiment. The normalization of array data to a subset of gene expression values was not performed because of the dramatic gene expression changes observed in RTT brain, including the differential expression of several genes usually considered to be "housekeeping" genes. Quantification of fluorescence data (UniGEM V and MICROMAX) entails the calculation of ratios and hence only one value per matched pair is depicted in Figs. 3 and 4. Extreme expression ratios resulting from near undetectable signal in one of the two fluorescence channels were limited to a maximum absolute value of 10 in their contribution to mean expression ratio values reported here.

Microarray data from CLONTECH were analyzed initially using AtlasImage software. Subsequently all microarray data were analyzed in Microsoft Excel as well as S-PLUS 2000 Professional (MathSoft, Inc.). Clustering algorithms in S-PLUS, PARTEK Pro 2000, and Michael Eisen's (Stanford University) Cluster and TreeView programs were used in the analysis of the Human Atlas Neurobiology Array dataset. Principal components analysis and multidimensional scaling algorithms within the PARTEK package were also used.

Subtractive Hybridization and cDNA Southern Blotting

Pools of total RNA from six RTT brains (R1–R6) and six control brains (C1–C6) were reverse transcribed to cDNA, digested with *Rsa*I, and subtracted using the PCR-Select cDNA Subtraction protocol (CLONTECH Laboratories, Inc.; www.clontech.com). Pools of differentially expressed cDNAs were subcloned into a TA-cloning vector (Invitrogen), and sequenced. The identity of clones was determined by BLAST searching with $=$99% nucleotide identity per 100 nucleotides used as a criterion. Five clones from each subtracted pool were sequenced. For Southern blot analysis, specific oligonucleotides corresponding to β-actin, α B-crystallin, and GFAP were used to PCR amplify transcripts from human brain cDNA (OriGene Technologies, Inc.). PCR products were sequenced, labeled with [α^{32}P]dCTP by random priming (RediPrime II, Amersham Pharmacia), and hybridized to nylon membranes containing pools of up- and down-regulated cDNAs generated by subtractive hybridization. For microarray analyses, pools of subtracted cDNAs were random prime labeled with [α^{33}P]dCTP and hybrid-

ized to Human GeneFilters (GF200 and GF202) from Research Genetics according to the manufacturer's protocol (www.resgen.com).

PCR, Immunoblotting, and Immunohistochemical Analyses

cDNA microarray results were independently confirmed by semiquantitative PCR to amplify specific products. Touchdown PCR conditions were used with a model PTC200 or a MiniCycler PCR machine (MJ Research). For each PCR, amplified product was evaluated by electrophoresis on agarose gels every three cycles from 24 through 36 to establish a linear range of amplification. Amplification of GAPDH was performed as a control. In all cases, quantification of RT-PCR results entailed subtraction of background signal and normalization to GAPDH levels.

Immunoblotting was performed using 10 or 20 μg of brain homogenate. Equal protein loading was confirmed by Ponceau S staining. Quantification of immunoblotting results entailed subtraction of background signal. Antibodies used for immunoblotting were directed against syntaxin 1A (monoclonal HPC-1, Sigma Chemical Co.), annexin VI (polyclonal, Santa Cruz Biotechnology, Inc.), or glial fibrillary acidic protein (GFAP; polyclonal, Chemicon).

Immunohistochemistry was performed on formalin-fixed, paraffin-embedded tissue (R1, R3, R6, 7 additional RTT cases, and 5 controls), using a polyclonal antibody against GFAP (DAKO) and the VECTASTAIN avidin–biotin complex kit (Vector Laboratories, Inc.).

RESULTS

Brain Tissue, MECP2 Mutations, and X Chromosome Inactivation Patterns

As animal models of RTT have only recently become available (Chen *et al.*, 2001; Guy *et al.*, 2001), the study of postmortem human brain tissue has been the primary method for the investigation of the molecular basis of neurological defects in RTT. In this report we study postmortem brain tissue exclusively. Postmortem female RTT brain samples were used for mRNA and protein expression studies (Methods; Table 1). Controls were age-, gender-, and brain region-matched. Dorsomedial cerebral cortex at the junction of the frontal and parietal cortices (Brodmann's areas 1–5) was dissected from each postmortem brain. The majority of cortical regions in RTT cerebral cortex show comparable neuropathology (Belichenko *et al.*, 1997; Kaufmann *et al.*, 1998).

We sequenced the *MECP2* coding region of genomic DNA derived from six RTT postmortem brains and identified mutations in four of the six individuals. All four mutations are single nucleotide substitutions consisting of C to T transitions and are predicted to result in a premature stop codon and truncation of the predicted MeCP2 protein in RTT cases R1, R2, R3, R5 (Fig. 1A). Two of these four mutations were identical to one another (Fig. 1A, cases R3 and R5). The three distinct mutations in the *MECP2* gene identified here have all been identified in other individuals in previous reports of *MECP2* mutations in RTT (Cheadle *et al.*, 2000). Our identification of *MECP2* coding region mutations in ~70% of RTT cases studied here is consistent with the percentage identified in larger patient populations (see Introduction). It is unclear whether the remaining patients harbor mutations elsewhere in the *MECP2* gene (promoter region, intronic sequence, or UTRs). The six RTT cases studied here represent a unified diagnostic group based both on clinical symptomology (S. Naidu) and transcriptional profiles (see *Molecular Classification of Rett Syndrome Patients* below).

Additional sequencing of cDNA reverse transcribed from brain mRNA revealed that both the intact and mutated copies of MeCP2 mRNA are transcribed in all RTT cases having identified mutations (Fig. 1B). This demonstrates for the first time that in RTT brain, *MECP2* is transcribed from both the intact and mutated X chromosomes in a mixture of brain cells. Hence, due to X inactivation patterns, each RTT case is a mosaic of wild-type and mutant MeCP2-expressing cells. In order to investigate the nature of this mosaic in each RTT case, we performed X chromosome inactivation studies on RTT brains samples (Fig. 1C). It is important to note that without analysis of parental DNA it is not possible to determine which of the alleles is paternal and which is maternal. Additionally, this analysis does not reveal which of the alleles is associated with the mutant MeCP2 allele (see Methods). Random pattern of X chromosome inactivation were observed in all cases studied. Although gene expression profiling was carried out on cerebral cortical samples, X inactivation was assessed in cerebellar tissue. For one of the RTT cases we assessed X chromosome inactivation in a second region of the CNS (spinal cord) and obtained identical results, consistent with the conclusion that X chromosome inactivation patterns in the CNS do not vary widely.

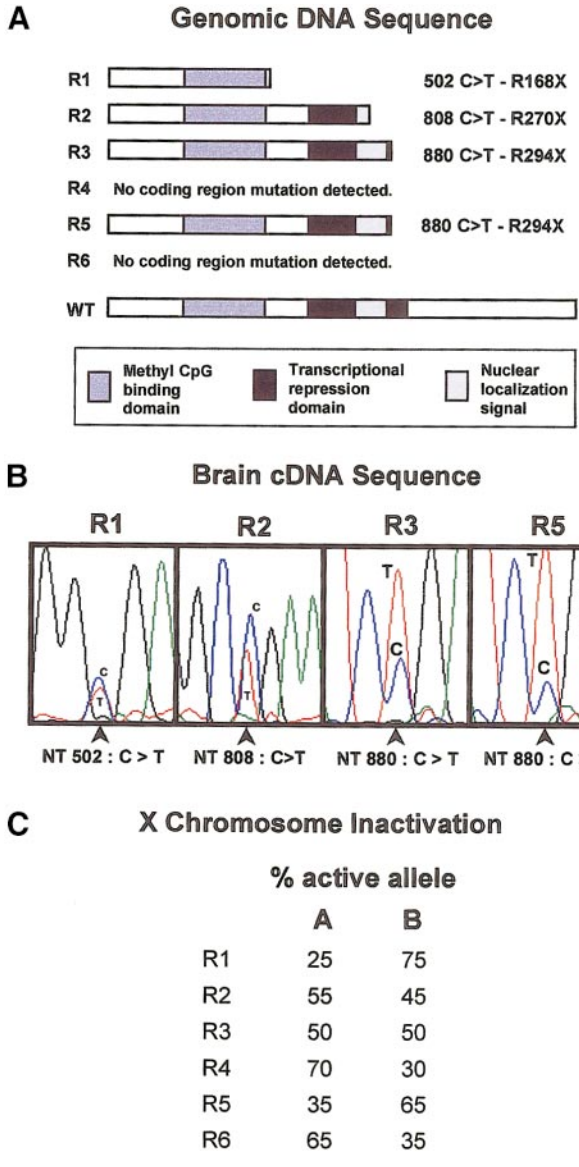

	A	B
R1	25	75
R2	55	45
R3	50	50
R4	70	30
R5	35	65
R6	65	35

FIG. 1. *MECP2* mutations identified in postmortem brain tissue. Mutations in the coding region of the *MECP2* gene were identified in genomic DNA derived from brain in four of the six RTT patients studied here. All four of the identified mutations were nonsense mutations resulting in a premature stop codon in the predicted mRNA sequence. Each of these four mutations and their predicted truncated protein products are detailed in A. In all of the four cases where *MECP2* mutations were found in genomic DNA, it was determined that both wild-type and mutant transcripts are expressed in brain via sequencing of cDNA derived from brain mRNA samples (B). X chromosome inactivation patterns were determined using genomic DNA derived from RTT cerebellar tissue (C).

Validation of Postmortem Samples and Gene Expression Analysis Methods

In order to ensure the highest quality of data would be acquired from the many expression analysis techniques used here, we first investigated the quality of RNA samples derived from the postmortem brain tissues. RNA purity was determined by monitoring the ratio of absorbance (A_{260}/A_{280}) in a spectrophotometer.

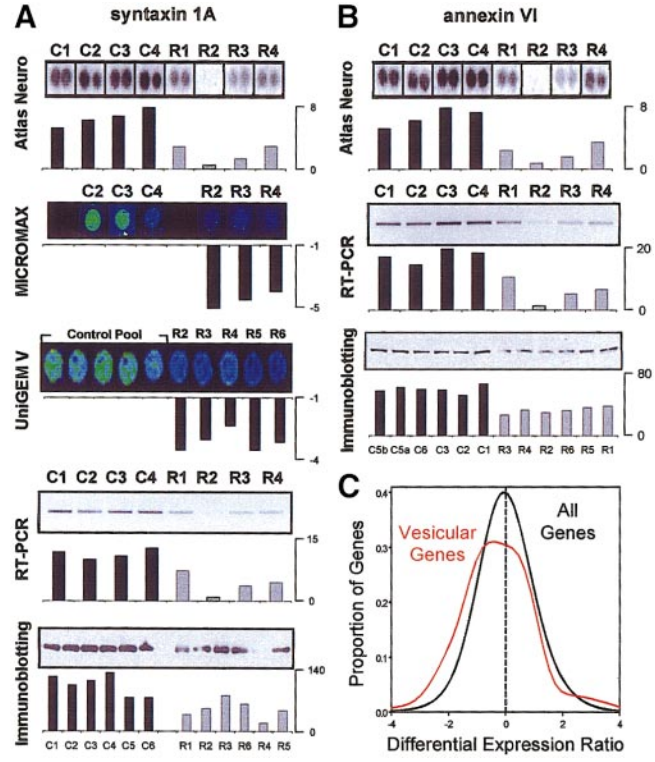

FIG. 3. Decreased expression of selected genes encoding presynaptic proteins in RTT brain. Decreased expression of syntaxin 1A was detected with the Human Atlas Array (A, first panel) and MICROMAX array (A, second panel). The UniGEM V array confirmed this result from an independent tissue sample and RNA extraction in samples R2-R4 and extended this finding to two additional cases R5 and R6 (A, third panel). These array findings were further validated by RT-PCR (A, fourth panel). Immunoblotting revealed a similar decrement in syntaxin 1A protein levels (A, fifth panel). Annexin VI expression was also shown to be decreased with the Human Atlas Array technology (B, first panel) and confirmed via RT-PCR (B, second panel). Immunoblotting demonstrated a similar decrease in annexin VI protein levels in all cases studied (B, third panel). The distribution of differential gene expression ratios associated with a subset of 35 genes identified as being localized to intracellular vesicles by the Swiss-Prot database (red, C) was compared to the distribution of differential gene expression ratios for all genes on the UniGEM V microarray (black, C). $N = 35$ genes (175 datapoints), $P < 2^* 10^{-8}$ as assessed by χ^2 analysis. Axes for CLONTECH, RT-PCR, and immunoblotting panels indicate arbitrary expression values after quantification of signal, subtraction of background, and normalization. Global normalization to the mean of all gene expression values was used for all CLONTECH data. Axes for UniGEM and MICROMAX fluorescent technologies indicate single expression ratios for each simultaneous hybridization (one value for each of the two images of the identical spot read through different fluorescent channels) after quantification of signal and global normalization.

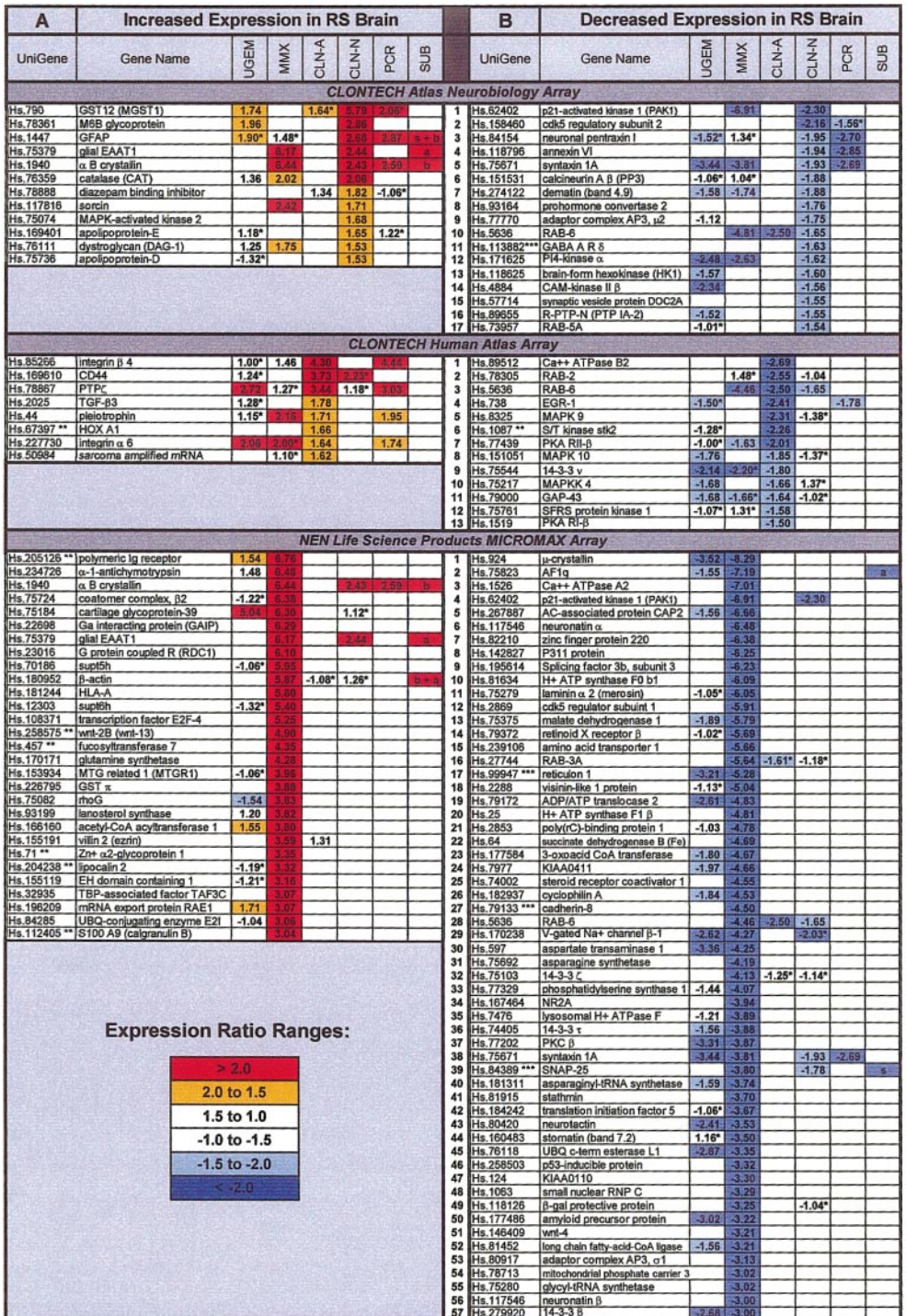

FIGURE 2

Integrity of RNA samples was confirmed by the identification of distinct ribosomal RNA bands and the absence of low molecular weight breakdown products using agarose gel electrophoresis. RNA quality was adequate to reliably allow reverse transcription and PCR amplification of control cDNAs including actin and tubulin. Only RNA samples which met all of these requirements were included in this study.

To confirm that array technologies could produce reliable results when applied to RNA samples derived from postmortem brain we first performed multiple array experiments using RNA derived from control brains. Gene expression profiles were generated for control brain tissue samples C1–C4 using Clontech Atlas Neurobiology Arrays. A mean Pearson's correlation coefficient, *r,* of greater than 0.97 was calculated for these expression profiles. This high level of correlation between datasets demonstrates the reproducibility of gene expression values across multiple (1) array experiments, (2) RNA preparations and labelings, and (3) control brain tissue samples. Similar cDNA microarray analyses have recently been successfully completed using postmortem brain tissue derived from subjects diagnosed with schizophrenia (Mirnics *et al.,* 2000; Hakak *et al.,* 2001; Mirnics *et al.,* 2001).

Differential Gene Expression: cDNA Microarray Analysis

We assessed gene expression in RTT and control brains using four independent cDNA microarray technologies: the Atlas Human cDNA array and the Atlas Human Neurobiology array (CLONTECH Laboratories, Inc.), the MICROMAX array (NEN Life Science Products, Inc.), and the UniGEM V 1.0 array (Incyte Genomics, Inc.). In addition to increasing the number of genes being investigated, the purpose of using multiple microarrays was to more reliably identify changes in gene expression and to cross-validate the results of the microarray technologies. Both CLONTECH arrays consist of 597 custom designed cDNAs spotted in duplicate on a nylon filter. mRNA from samples R1–R4 and C1–C4 was used to generate radiolabeled cDNA probes for individual hybridization to replicate Atlas arrays. MICROMAX arrays contain 2400 cDNA elements corresponding to known human genes. Total RNA from RTT samples R2–R4 and matched controls C2–C4 was reverse transcribed and haptenated probes generated for simultaneous hybridization of individual RTT-control pairs to MICROMAX arrays followed by sequential deposition of Cyanine 3 and Cyanine 5 Tyramide fluorescence. A single tissue sampling and RNA preparation was used for all CLONTECH, MICROMAX, and subsequent RT-PCR analyses. UniGEM V array analysis was conducted on a distinct mRNA preparation from an independent tissue sampling of RTT samples R2–R6 and controls C1–C6. mRNAs from controls C1–C6 were pooled and compared to individual RTT samples R2–R6 in five independent simultaneous fluorescent hybridization experiments employing the UniGEM V microarray technology representing ~7000 human genes. In this report we have used the UniGEM V expression data primarily to confirm changes identified with the other technologies (a more complete analysis of this dataset is underway by Colantuoni *et al.,* in preparation). Background subtraction and global normalization procedures were applied to all datasets in order to make results as accurate and comparable across the multiple technologies as possible (see Methods for details).

To identify genes consistently differentially expressed in RTT brain, several criteria were applied in the analysis of cDNA microarray data: (1) Clear and reliable image acquisition suitable for quantification (determined by manual image inspection and automated image quantification). (2) Minimum expression level required for reliable quantification of signal (CLONTECH: 75% of mean array element signal in-

FIG. 2. Genes most consistently and most differentially expressed in RTT brain. Genes with increased expression in RTT are depicted in A, and genes with decreased expression in RTT are depicted in B. Genes fulfilling criteria described in the text are listed by UniGene number and gene name at the left of each panel and are ordered by magnitude of differential expression. Expression ratios as assessed by the various cDNA array technologies (UGEM, MMX, CLN-N, CLN-A), reverse-transcription polymerase chain reaction (PCR), and cDNA subtraction (SUB) are listed in columns to the right. All gene expression values are expressed in ratios relative to matched controls (see Table 1 for subject details) and are color coded to reflect magnitude of differential gene expression. Gene expression changes of magnitude less than 1.5-fold are not colored as they do not represent reliable and significant expression changes. An asterisk indicates that expression ranges were not nonoverlapping. Blank cells indicate the gene of interest was not assessed by a particular technology. Abbreviations: UGEM, UniGEM V microarray; MMX, MICROMAX; CLN-A, CLONTECH Human Atlas array; CLN-N, CLONTECH Atlas Neurobiology array; PCR, results of PCR experiments; SUB, results of subtractive hybridization experiments; Abbreviations for techniques used to identify cDNAs from subtracted cDNA pools: s, sequencing; b, cDNA southern blot; a, probing of Human GeneFilter arrays with subtracted cDNA pools.

tensity; MICROMAX: 50% of mean array element signal intensity). (3) Consistent differential expression across all samples studied: (3A) Nonoverlapping expression value ranges for the RTT and control groups. In a non-overlapping expression pattern for a given gene, all disease cases have expression values greater than all or less than all control cases. (3B) A Student's *t* test with a *P* value of less than 0.10. This less stringent p value was used because it is only one of three consistency criteria applied to the data. (3C) A minimum differential expression ratio for each of the individual subject comparisons: CLONTECH: ± 1.0; MICROMAX: ±2.0. (4) Magnitude of differential expression. CLONTECH: mean expression ratios with an absolute value of 1.5 or greater. MICROMAX: mean expression ratios with an absolute value of 3.0 or greater. These ratio values represent greater than 2.0 standard deviations from the mean expression ratio in all three of the microarray datasets.

Figure 2 depicts the most consistently and dramatically differentially expressed genes in RTT brain as determined by each microarray technology ordered by magnitude of differential expression (increases, Fig. 2A; decreases, Fig. 2B). Each data point in Fig. 2 fulfills each of the criteria listed above. Hence, the reported changes in gene expression were consistent across multiple independent RTT patients, tissue samplings, and RNA preparations. The genes listed in Fig. 2 account for 4.9% of the genes contained on the Atlas Neurobiology array, 3.4% of the genes contained in the Human Atlas array, and 3.6% of the genes on the MICROMAX array. Gene expression results were highly consistent across multiple microarray technologies, as shown in Fig. 2. In several cases, differences in gene expression between RTT and control samples were confirmed using RT-PCR with primers identical to those used to generate the cDNAs spotted on the Atlas arrays. In 12 of 14 cases, semiquantitative RT-PCR analyses independently confirmed the microarray results (Fig. 2, PCR columns). Results obtained from subtractive hybridization are also consistent with microarray results and are included in Fig. 2, SUB columns (see *Differential Gene Expression: Subtractive Hybridization* below).

When these uniform criteria were applied to datasets derived from all four microarray technologies used here, a greater number of genes were found to be consistently down-regulated than were found to be consistently up-regulated in RTT brain. It is unlikely that this finding is due to the preferential identification of down-regulated genes as global normalization processes in the analysis of the expression data ensure that for each RTT: Control comparison an equal number of genes are identified as up- and down-regulated. The identification in Fig. 2 of a greater number of genes with decreased expression in RTT brain appears to stem from the greater consistency of genes found to be down-regulated than those found to be up-regulated. That is, the genes found to have decreased expression in individual RTT cases are more often the same genes across multiple cases, while the set of genes with increased expression varies more greatly across RTT cases. We are currently assessing the statistical validity and biological significance of this finding (Colantuoni *et al.*, in preparation).

Differential Gene Expression: Neuronal Transcripts

Inspection of this list of most consistently and differentially regulated genes (Fig. 2) reveals several genes that are of particular interest as they appear to delineate cellular pathways and components that may be involved in RTT neuropathology. Consistent with the previously documented disruption of neuronal maturation is the finding that many transcripts that are specific to or enriched in neurons show decreased expression in RTT brain tissue: neuronal pentraxin 1, calcineurin, GABA and glutamate receptors, CAM kinase II β, neuronal olfactomedin-related ER localized protein (NOEL), two Ca^{2+} ATPases, neuronatin α and β, neuron specific enolase, and PCP4 (Fig. 2B). Although not listed in Fig. 2, several other neuronal cDNAs were found to be down-regulated in RTT brain by 50% or more: AMPA receptors 1 and 2, GABA A β3 receptor, neurofilament proteins of 66 and 200 kDa, MAP-2, MAP-1B, tau, and tau kinase II (UniGene identifiers: Hs.7117, Hs.89582, Hs.1440, Hs.76888, Hs.198760, Hs.167, Hs.103042, Hs.101174, Hs.2869; MICROMAX and UniGEM V data not shown). Despite this apparent global down-regulation of neuronal transcripts, a number of such cDNAs were found to be enriched by at least 50% in RTT brain: NR1, AMPA receptor 3, mGluR1, mGluR8, and GABA A receptor π (UniGene identifiers: Hs.105, Hs.100014, Hs.32945, Hs.86204, Hs.70725; MICROMAX and UniGEM V data not shown).

Further inspection of gene expression changes in RTT brain indicates that in addition to a general reduction in neuronal maturation and structural transcripts, the expression of genes encoding presynaptic markers are impacted in particular: annexin VI, syntaxin 1A, DOC2A, and synaptosomal-associated protein of 25 kDa (SNAP-25; Fig. 2B). Four different members of the 14–3–3 gene family were demonstrated to be consistently under-expressed in all RTT cases stud-

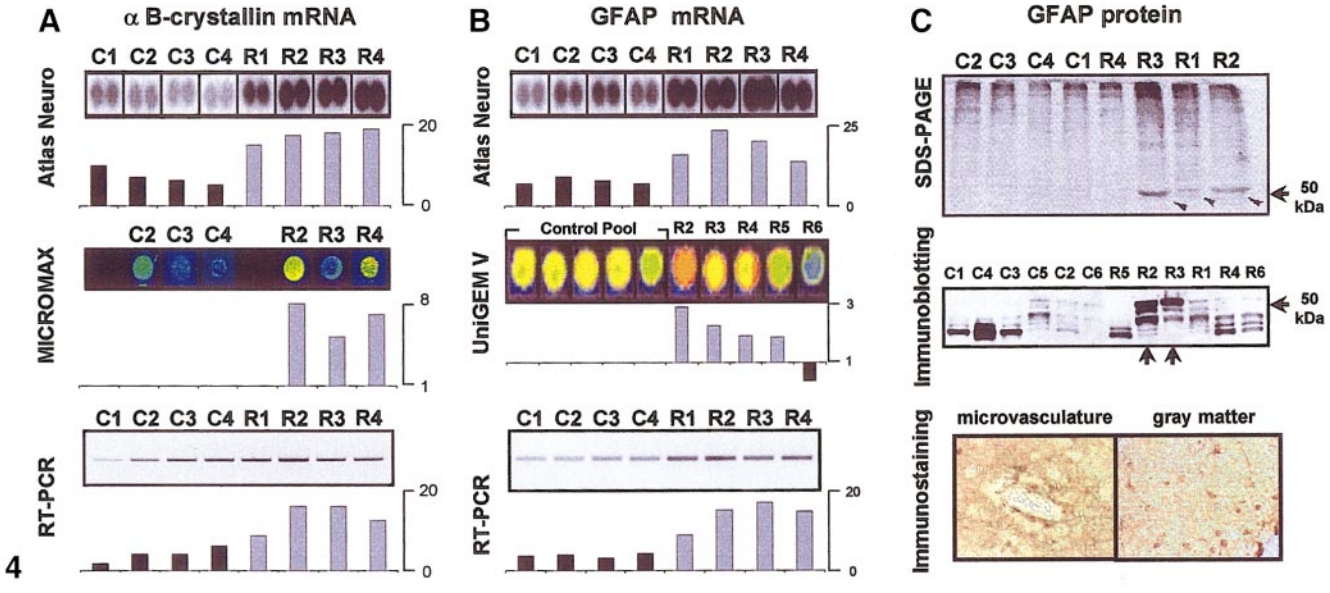

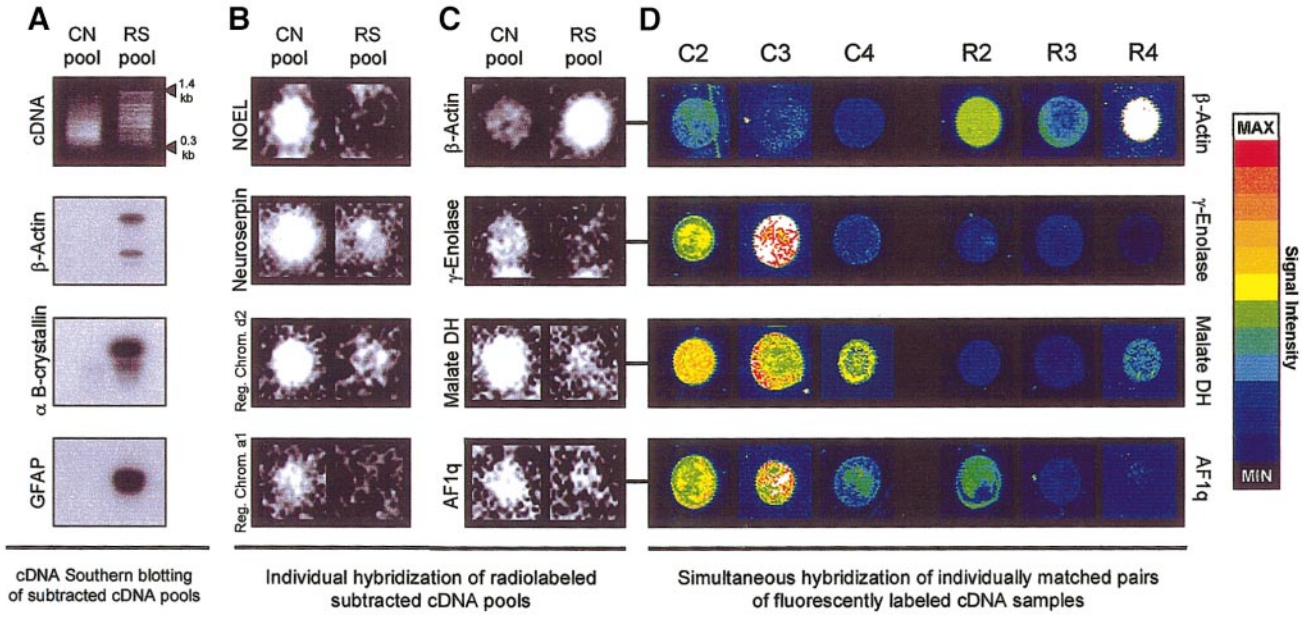

FIG. 4. Increased expression of selected glial genes in RTT brain. Elevated mRNA expression of α B-crystallin was detected with the Human Atlas Neurobiology Array (A, top panel) and the MICROMAX array technologies (A, middle panel). This finding was confirmed using RT-PCR (B, bottom panel). Increased GFAP expression was detected with the Human Atlas Array (B, top panel) and confirmed via RT-PCR (B, bottom panel). From experiments using an independent tissue sampling and RNA extraction, the UniGEM V array confirmed increased expression in cases R2–R4 and reveled increased expression in case R5, but a slight decrease in case R6 (B, middle panel). 52-kDa protein stained with Coomassie brilliant blue that remained in polyacrylamide gels after electrophoretic transfer of RTT brain proteins to membranes for immunoblotting (C, top panel). Protein microsequencing determined this protein to be 97% identical to the amino acid sequence of human GFAP (GenBank Accession No. NP_002046). Immunoblotting confirmed that this band was the heaviest migrating form of GFAP (C, middle panel). Both immunoblotting and immunohistochemistry revealed varying levels of GFAP protein expression in the RTT cases (C, middle and bottom panels). High levels of GFAP immunoreactivity were often observed near brain microvasculature and within gray matter (C, bottom panel; case R1 shown). Axes for CLONTECH, RT-PCR, and immunoblotting panels indicate arbitrary expression values after quantification of signal, subtraction of background, and normalization. Global normalization to the mean of all gene expression values was used for all CLONTECH data. Axes for UniGEM and MICROMAX fluorescent technologies indicate single expression ratios for each simultaneous hybridization (one value for each of the two images of the identical spot read through different fluorescent channels) after quantification of signal and global normalization.

FIG. 5. cDNA subtraction. RNA samples from RTT cases R1–R6 were pooled as were control cases C1–C6. cDNA subtraction was performed to generate pools of subtracted cDNAs up-regulated in RTT (right lanes / spots in A, B, and C) and transcripts expressed at low levels in RTT (left lanes / spots in A, B, and C). Ethidium bromide staining of cDNA from both pools after electrophoresis through an agarose gel confirmed the presence of intact, heterogeneous populations of cDNAs. Differential abundance of β-actin, α B crystallin, and GFAP cDNAs was demonstrated by cDNA southern blotting (A). This was primarily a validation of the cDNA subtraction, as increased expression of these transcripts had already been determined using cDNA microarrays (C, Figs. 2B, 4A, and 4B). Subtracted cDNA pools were used for the

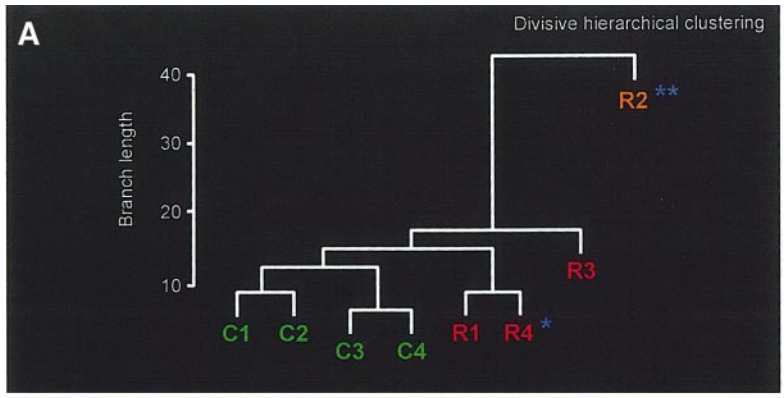

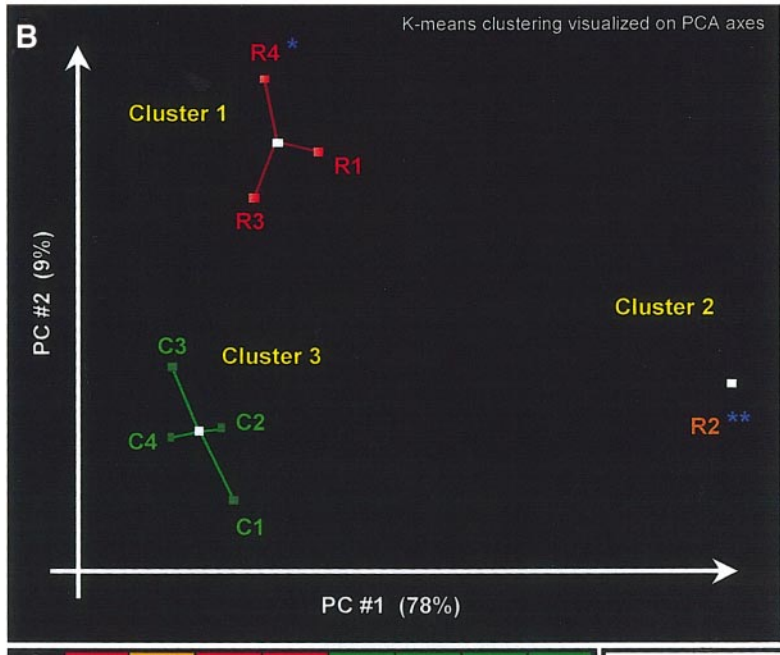

C

Pearson's correlation matrix

	R1	R2	R3	R4	C1	C2	C3	C4
R1	1.000							
R2	0.789	1.000						
R3	0.946	0.846	1.000					
R4	0.972	0.785	0.943	1.000				
C1	0.956	0.772	0.943	0.930	1.000			
C2	0.970	0.746	0.924	0.950	0.976	1.000		
C3	0.948	0.681	0.898	0.939	0.953	0.974	1.000	
C4	0.943	0.684	0.901	0.924	0.964	0.976	0.985	1.000

Mean Correlation Coefficients

0.954	Within RS Cluster
0.880	Wthin RS Cluster (W/ R2)
0.806	R2 : RS Cluster
0.721	R2 : Control Cluster
0.971	Within Control Cluster
0.935	Between Clusters
0.901	Mean of All Correlations

FIG. 6. Multiple cluster analyses of gene expression profiles. Divisive hierarchical clustering of control (C1–C4) and Rett Syndrome (R1–R4) samples using CLONTECH Atlas Neurobiology Array data in S-PLUS analysis software (A). K-means clustering using CLONTECH Atlas Neurobiology data in PARTEK analysis software. Axes are derived from principal components analysis (B). By comparing each individual gene expression value between pairs of subjects, a matrix of Pearson correlation coefficients was generated (C). An asterisk indicates no mutation within the coding region of the MECP2 gene was identified in this subject. Two asterisks indicate severe agonal state of subject R2. Percentages associated with the PC axes indicate the percentage of variance accounted for by that PC axis.

---

generation of ^{33}P-labeled probes and hybridized to Research Genetics' Human Gene Filters (GF200 and GF202). The differential expression of two genes already identified via sequencing of subcloned cDNAs from subtracted pools was confirmed (NOEL and neuroserpin; B, top two panels). The abnormal expression of two genes involved in transcriptional control was revealed (regulators of chromatin d2 and a1; B, bottom two panels). Four other genes displaying differential abundance in the subtracted pools were discovered by probing Human GeneFilters with labeled cDNA derived from subtracted cDNA pools: β-actin, γ-enolase, cytosolic malate dehydrogenase, and transmembrane protein AF1q (C). The differential expression of these four genes was validated by data acquired via the simultaneous hybridization of individual control and RTT cDNA probes performed independently with the MICROMAX array system (D). Abbreviations: Rett Syndrome (RTT); Control (CN).

ied (Fig. 2B). This is of particular interest as several 14–3–3 proteins have key roles in neural development (Skoulakis and Davis, 1998). Moreover, multiple members of the 14–3–3 family, including several of those listed in Fig. 2B, have been demonstrated to localize to presynaptic membranes (Martin *et al.*, 1994; Jones *et al.*, 1995) and regulate learning and presynaptic function (Broadie *et al.*, 1997; Zhou *et al.*, 1999). Also interesting is the decreased expression of protein kinase C (Fig. 2B), which has extensive interactions with several of the 14–3–3 proteins (Hausser *et al.*, 1999; Van Der Hoeven *et al.*, 2000).

The differential expression of two presynaptic markers, the synapsin binding protein annexin VI (Inui *et al.*, 1994) and syntaxin 1A, was investigated in further detail (Fig. 3). Decreased mRNA expression of both genes was confirmed using the multiple cDNA array technologies in addition to semi-quantitative RT-PCR. Decreased protein expression of both of these genes was discovered using standard western blotting techniques. Additional presynaptic markers showing reduced expression of at least 50% included the following: synaptophysin, synapsin II, synaptogyrins 1 and 3, synaptotagmins 1 and 5, synaptobrevin 2, and NSF (UniGene identifiers: Hs.75667, Hs.6439, Hs.6139, Hs.6467, Hs.154679, Hs.23179, Hs.194534, Hs.108802; MICROMAX and UniGEM V data not shown).

Additional evidence for the disruption of presynaptic development in RTT brain was discovered through the investigation of the distribution of differential expression ratios associated with genes that encode vesicular proteins (Fig. 3C). Using the DRAGON database (Bouton and Pevsner, 2000); (http://pevsnerlab.kennedykrieger.org/dragon.htm), we identified every gene in our UniGEM V dataset defined in the Swiss-Prot database as being localized to intracellular vesicles. 35 of the 7075 genes included in the UniGEM V dataset were included in this classification, resulting in a total of 175 datapoints: 35 genes * 5 RTT cases investigated with the UniGEM V system = 175 differential gene expression ratios. The distribution of differential gene expression ratios associated with this subset of 35 genes was compared to the distribution of all differential expression ratios (5 RTT cases * 7075 genes in the UniGEM V array = 35375 datapoints) using standard χ^2 analysis. The expression of genes encoding vesicular proteins was found to be significantly decreased relative to the expression of other genes on the array (Fig. 3C). We believe that this reflects a general decrease in the expression of genes required for presynaptic neurotransmitter release associated with the decreased number of synapses previously described in RTT brain (Jellinger *et al.*, 1988; Bauman *et al.*, 1995a; Belichenko *et al.*, 1997).

Differential Gene Expression: Glial Transcripts

Several genes encoding glia-specific proteins showed increased expression in RTT brain, including α B-crystallin, glial fibrillary acidic protein (GFAP), glial exictatory amino acid transporter 1 (EAAT1), and S100 A13 (Fig. 2A). The increased expression of both α B-crystallin and GFAP was confirmed by multiple array technologies, RT-PCR, and cDNA subtraction (Figs. 2A, 4A, 4B, and 5A).

GFAP protein levels were also found to be dramatically increased in RTT cases (Fig. 4C). In independent biochemical studies of RTT brains, we observed a prominent protein of 52 kDa stained with Coomassie brilliant blue that remained in polyacrylamide gels after electrophoretic transfer of RTT brain proteins to membranes for immunoblotting (Fig. 4C, top panel). We subjected the 52-kDa protein to tryptic digestion, mass spectrometry using matrix assisted laser desorption/ionization time of flight (MALDI-TOF), reverse phase high pressure liquid chromatography, and automated microsequencing of tryptic fragments. BLAST searches revealed that the obtained sequences for the two major peptides (QQVHVELDVAKPDLTAALK and TGYEAMASSNMHEAEEWY) shared 97% sequence identity with human GFAP (GenBank Accession No. NP_002046). Immunoblotting confirmed that this band was the heaviest migrating form of GFAP (Fig. 4C, middle panel). The levels of this heaviest form of GFAP were highest in RTT cases in which the highest mRNA levels were detected (R2 and R3). Both immunoblotting and immunohistochemistry revealed varying levels of GFAP protein expression in the RTT cases (Fig. 4C, middle and bottom panels). High levels of GFAP immunoreactivity were often observed within the gray matter of RTT brain tissue (Fig. 4C, bottom panel). Gray matter gliosis of this nature is highly uncommon in control individuals.

Previously, overexpression of GFAP and gliosis have been reported in some RTT cases (Jellinger and Seitelberger, 1986; Jellinger *et al.*, 1988; Oldfors *et al.*, 1988, 1990; Ahlsen *et al.*, 1993; Bauman *et al.*, 1995a; Kaufmann *et al.*, 1995; Deguchi *et al.*, 2000). In addition, an increase in astrocyte-associated gangliosides has been described in RTT cerebral cortex (Lekman *et al.*, 1991). Several other genes implicated in neurodegeneration and astroglial reactivity were also found to have increased expression in RTT brain, including HSP27(UniGene Identifier: Hs.76067, data not shown),

apolipoprotein-E (Fig. 2A), and apolipoprotein-J (UniGene identifier: Hs.75106, data not shown).

Differential Gene Expression: Subtractive Hybridization

To measure changes in gene expression in RTT brains using an independent technique, we performed cDNA subtraction. Pools of total RNA from RTT brains R1–R6 and control brains C1–C6 were reverse transcribed, differentially subtracted, and amplified using the CLONTECH PCR-Select cDNA Subtraction protocol. Five clones from each subtracted pool were sequenced (Fig. 2, bottom panel). Among the clones sequenced from the pool of cDNAs with increased expression in RTT brain was the glial gene GFAP (Fig. 2A). Several neuronal transcripts were sequenced from the pool of cDNAs with decreased expression in RTT brain, including neuroserpin, NOEL, and SNAP-25 (Fig. 2B). Both GFAP and SNAP-25 had been previously identified as differentially expressed with microarray analysis (Fig. 2 and 4B). The identification of the non-human hepatitis C virus cDNA (Fig. 2A) is thought to be the result of an undiagnosed hepatitis infection in one of the six RTT subjects included in the pool of cDNAs used for subtraction.

cDNA southern blotting was used to confirm the differential presence of three transcripts already identified as differentially expressed in RTT brain: β-actin, α B-crystallin, and GFAP (Fig. 2A). These three transcripts were detected selectively in the pool of cDNAs overexpressed in RTT (Fig. 5A), indicating that microarray and subtractive hybridization approaches yielded consistent results. Finally, in order to further cross-validate the microarray and subtractive hybridization approaches and to identify additional differentially expressed cDNAs present in the subtracted pools, the subtracted cDNA pools were used to generate radiolabeled probes for use with Research Genetics Human GeneFilter arrays (Figs. 2, 5B, and 5C). This resulted in the confirmation of differential expression of cDNAs we had identified through sequencing of clones in the subtracted pools: NOEL and neuroserpin (down-regulated, Fig. 5B) and β-actin (up-regulated, Fig. 5C). Probing of microarrays with the subtracted pools also revealed the differential expression of genes not previously identified (Fig. 2A and 2B, bottom panels indicated with "a"). Two such examples are pictured in Fig. 5B, showing the decreased expression of two genes encoding regulators of chromatin d2 and a1. Additional genes involved in general chromatin structure regulation were found to be differentially expressed with microarray technologies, including supt5h and supt6h (up-regulated, Fig. 2A) and regulators of chromatin b1, c2 (decreased expression; UniGene identifiers: Hs.159971 and Hs.236030; data not shown), d3, and a3 (increased expression; UniGene identifiers: Hs.77069 and Hs.3068; data not shown). Several genes identified as differentially expressed based on analysis of GeneFilters probed with the subtracted cDNA pools (Fig. 5C) were also observed to be abnormally expressed according to independent MICROMAX microarray experiments using individual brain RNA samples (β-actin, neuron-specific enolase, cytosolic malate dehydrogenase, AF1q; Fig. 5D and Fig. 2).

Differential expression findings with the microarray technologies cross-validated well with the results obtained from these three different methods of identifying transcripts present in the subtracted cDNA pools (Fig. 2). The subtractive hybridization findings again confirm the pattern of increased glial reactivity and impaired neuronal and presynaptic development in RTT brain that had been concluded from the microarray analysis. cDNA subtraction revealed the increased expression of several glial-specific transcripts, including GFAP, α B crystallin, and the glial EAAT1, and the decreased expression of many neuronal transcripts including neuroserpin, NOEL, SNAP-25, and neuron-specific enolase.

Molecular Classification of Rett Syndrome Patients

We performed cluster analysis to determine which postmortem brain cases resemble each other in overall patterns of gene expression. The goal of this analysis was to distinguish RTT samples from matched controls based solely on profiles of gene expression in brain. Several clustering algorithms were applied to the Atlas Human Neurobiology dataset of 597 gene expression values. Using the statistical software S-Plus 2000, we employed a divisive hierarchical clustering algorithm to generate a clustering tree which accurately segregated RTT from control samples based solely on gene expression profiles in brain (Fig. 6A). Several other algorithms also yielded virtually identical clustering trees or cluster assignments, including the agglomerative clustering algorithm in Cluster (Micheal Eisen, Stanford University), K-means clustering, fuzzy partitioning, and partitioning around medoids (S-PLUS). The PARTEK Pro 2000 analysis package was used to apply both minimum variance (data not shown) and K-means clustering (Fig. 6B) to this

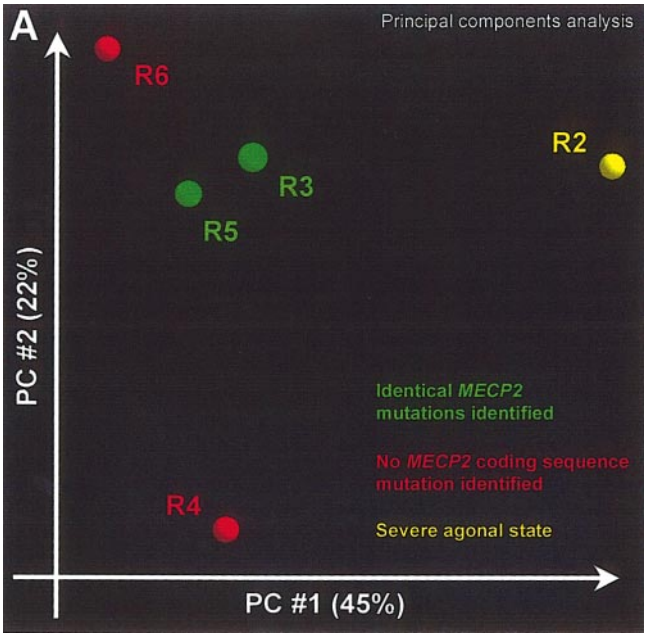

FIG. 7. Principal components analysis (PCA) of gene expression profiles within the RTT diagnostic group. PCA within the PARTEK analysis package was applied the set of 7075 differential gene expression values generated with the UniGEM V microarray system. Percentages associated with the PC axes indicate the percent of variance accounted for by that PC axis.

same dataset and again distinguish RTT from control samples. Subject R2 was identified as an outlier in both the clustering trees (Figs. 6A and 6B) and cluster assignments generated by the various algorithms (data not shown). Prior to death, this patient experienced cardiac arrest, remained unconscious with an extreme fever, and was maintained on life-support for the final 8 days of her life. An individual's agonal state can influence gene expression profoundly (Colantuoni *et al.*, 2000), and this may be reflected in the clustering tree. When limited to 2 clusters, all these algorithms assign R2 to its own cluster while all other subjects fall into a second cluster. When limited to 3 clusters R2 is again in its own cluster, and the remaining two clusters divide RTT and control individuals accurately. In general, the clustering algorithms found that three clusters best minimized within-cluster variance while maximizing between-cluster variance. In addition to displaying the results of the K-means clustering, which is depicted by the white cluster centers and colored cluster members, Fig. 6B shows the results of principal components analysis (PCA). The position of each subject in space is defined by the principal components derived from this analysis. This again makes clear that subject R2 is an outlier and that the other RTT subjects cluster tightly together as do the control subjects.

By pair-wise comparison of all subjects studied with the CLONTECH Atlas Neurobiology array, we generated a matrix of Pearson correlation coefficients (Fig. 6C). The mean correlation for all expression profiles was slightly greater than 0.9, however, mean correlation coefficients within and between the various clusters varied widely. Between cluster comparisons yielded a mean correlation coefficient of 0.935, while both within cluster coefficients were greater than 0.950. This indicates that the two clusters show a high degree of internal similarity. Additionally, correlation within the control cluster was greater than that within the RTT cluster, demonstrating that there is less variance within the control cluster. Each of the seven lowest correlation coefficients belonged to subject R2, again confirming this case as an outlier.

Each individual brain sample (R1–R4 and C1–C4) was hybridized to a single CLONTECH Atlas Human Neurobiology Array, facilitating the comparison of expression profiles across both RTT and Control groups (Fig. 6). A different experimental design was used in the UniGEM V microarray analysis. In five distinct simultaneous two-color hybridization experiments, mRNA from each of the five individual RTT brain samples (R2–R6) was compared to a single control mRNA pool (pooled cases C1–C6). As each of the RTT cases was compared to the identical control pool, this design is ideal for the examination of variance across gene expression profiles within the RTT diagnostic group. Figure 7 depicts principal components analysis of the 5 RTT gene expression profiles generated with the UniGEM v microarrays. Subject R2 is again a clear outlier in the group, lying distant from the other four cases along the principal component (PC) axis, which accounts for the greatest proportion of variance in these gene expression profiles (PC No. 1 accounts for 45% of the variance in these datasets). Cases R3 and R5 lie closer to one another than any other of the RTT cases, demonstrating that their gene expression profiles share more similarity than do any of the other cases. Cases R3 and R5 were found to harbor identical *MECP2* mutations (880 C > T; Figs. 1A and 1B). This correlation of genotype with gene expression profile demonstrates that high throughput expression analysis in complex tissues may be useful not only in the diagnosis of human disease, but also in the subcategorization of individual patients within a single diagnostic group.

DISCUSSION

Specific Changes in Gene Expression

In the present study we measured the expression of thousands of genes in postmortem human brain of patients with a clinical diagnosis of RTT. These patients harbored a number of different mutations in the *MECP2* gene, as well as different patterns of X chromosome inactivation. We have demonstrated that high quality RNA from postmortem brain tissue can be reliably extracted and assayed. The use of multiple cDNA microarray technologies, subtractive hybridization, RT-PCR, and protein biochemistry, allowed the cross-validation of biological samples as well as experimental methods.

The observed reductions in the mRNA expression and protein levels of many presynaptic markers are most likely directly linked to the reduced number of identifiable synapses in RTT brain. This is consistent with previous neuropathological studies detailing a reduction in neuronal cell volumes, dramatically decreased dendritic arborization, and a reduced number of identifiable synapses and dendritic spines in RTT brain (Jellinger *et al.*, 1988; Belichenko *et al.*, 1994; Bauman *et al.*, 1995a,b; Belichenko *et al.*, 1997; Kaufmann *et al.*, 1997). Also consistent with this disruption of synapse development is the magnetic resonance spectroscopic finding of reduced regional concentrations of *N*-acetyl aspartate (NAA) in white and gray matter of frontal and parietal cortices in RTT patients (Horska *et al.*, 2000). The extensive reductions in the expression of presynaptic markers observed here suggest that the disruption of neuronal development in RTT may be primarily presynaptic. Further evidence for the specificity of a presynaptic deficit in RTT is the increased or unchanged expression of several postsynaptic neuroreceptors discussed in the RESULTS above.

Increases in both α B-crystallin (Lowe *et al.*, 1992b, 1992a, 1993) and GFAP (Norton *et al.*, 1992; Laping *et al.*, 1994; Wu and Schwartz, 1998) expression have been identified in numerous CNS disease and injury paradigms other than RTT. α B-crystallin overexpression has been found in a wide range of neurological disease involving neuronal degeneration, including Alzheimer (Renkawek *et al.*, 1994), Parkinson (Renkawek *et al.*, 1999; Jellinger, 2000), and Huntington (Jackson *et al.*, 1995) diseases. It has been identified as a component of glial Rosenthal fibers (Iwaki *et al.*, 1989) that are present in the brains of individuals with Alexander's disease and other disorders involving chronic gliosis. Overexpression of GFAP in transgenic mouse models causes the formation of Rosenthal fibers in astrocytes (Eng *et al.*, 1998; Messing *et al.*, 1998). Several genes found to be up-regulated in RTT brain, including GFAP, α B-crystallin, HSP27, and ubiquitin have all been detected in Rosenthal fibers (Goldman and Corbin, 1991; Tomokane *et al.*, 1991; Head *et al.*, 1993; Iwaki *et al.*, 1993). Several other genes found to have increased expression in RTT brain have been implicated in neurodegeneration and astroglial reactivity, including HSP27 (Iwaki *et al.*, 1993), apolipoprotein-E (Corder *et al.*, 1993; Tomimoto *et al.*, 1997), and apolipoprotein-J (Matsubara *et al.*, 1995; Oda *et al.*, 1995; Boggs *et al.*, 1996; Choi-Miura and Oda, 1996; Matsubara *et al.*, 1996). Given the lack of specificity of GFAP and α B-crystallin overexpression, the abnormal expression of this group of genes most likely represents part of a transcriptional program underlying a common cellular pathology that is involved in, but not specific to, RTT neuropathology.

Although a number of the gene expression changes observed in RTT brain are most likely common to many neuropathological conditions, additional data acquired from autistic brain samples indicates that many expression changes may be specific to RTT. We compared gene expression patterns in autistic brain samples to that in matched control samples using the CLONTECH Atlas Neurobiology Arrays (Purcell *et al.*, in press). We used a region of the brain which is highly affected in RTT for expression analysis in RTT. Similarly, we selected a brain structure which has been previously implicated in the pathology of autism for the study of gene expression in this disorder. Cerebellar tissue samples were acquired from six autistic brain samples as well as six matched controls. Hence, both the RTT and autism studies sought to identify genes differentially expressed in regions of the brain affected in the respective disorders. Only one of the $>$150 genes included in Fig. 2 (i.e., genes differentially expressed in RTT brain) were found to be differentially expressed in the autistic brain samples: Hs.75379, the glial glutamate transporter EEAT1. From a global perspective, expression changes in the brains of individuals diagnosed with autism, a disorder sharing several clinical features of RTT, do not resemble gene expression changes observed in the brains of individuals with RTT.

In summary, individual changes in gene expression indicated a clear disruption of presynaptic development and increased astroglial reactivity in RTT brain. The changes in the expression of neuronal- and glial-specific genes constitute a proof-of-principle experiment, demonstrating the feasibility of high through-

put gene expression analysis in human postmortem brain tissue by paralleling previous neuropathological studies. The gene expression changes we have characterized here are a molecular portrait of the transcriptional programs underlying neuropathology that has been observed for years.

Molecular Classification of Patients

The ability to distinguish RTT from control cases using only brain gene expression profiles is a significant advance. Accurate molecular classification of diseased biological samples employing gene expression profiling, although previously achieved in cancers (DeRisi *et al.*, 1996; Khan *et al.*, 1998; Alizadeh *et al.*, 1999; Golub *et al.*, 1999; Khan *et al.*, 1999; Perou *et al.*, 1999; Wang *et al.*, 1999; Bittner *et al.*, 2000; Elek *et al.*, 2000; Perou *et al.*, 2000; Ross *et al.*, 2000; Xu *et al.*, 2000) has not been successful in complex human tissues such as brain. The successful classification of RTT patients here demonstrates that disease-specific patterns of gene expression can be identified in complex tissue sources and may be used for the diagnosis of human diseases. While routine molecular diagnosis of individuals via gene expression profiling in brain is unrealistic, the ability to segregate disease samples from controls will be useful in future applications to other disorders if a similar process can be applied to peripheral tissues such as muscle, skin, or blood. If the acquisition of CNS tissue is required, the collection olfactory receptor neurons via nasal biopsy may be a possibility.

The finding that gene expression profiles in brain can be used to meaningfully segregate individuals within the RTT diagnostic group with respect to *MECP2* genotype demonstrates that in addition to being useful in the diagnosis of human disease, such transcriptional analysis is likely to become useful in the sub-categorization of patients within a single diagnostic group. This information could be implemented in the development and application of more effective, individualized therapeutic strategies.

Issues in the Study of Rett Syndrome

The majority of clinically diagnosed RTT cases are caused by mutations in *MECP2*. A critical issue is to define specific genes that are differentially expressed in this disease as a direct consequence of the expression of a mutant *MECP2* gene. It is also particularly important that this analysis be done in the brain because, although MeCP2 mRNA is expressed throughout the body, the RTT phenotype is primarily neurological. A number of key genes may be over expressed in brain at critical times during RTT brain development, causing a complex cascade of abnormal gene expression and neuropathological events. Gene expression profiling in postmortem RTT brain samples allows the analysis of gene expression at a time which is usually long after this initial insult. Hence, many of the observed changes in gene expression may be reflective of gross cellular and histological differences - a molecular characterization of RTT neuropathology rather than etiology.

For many brain diseases, including RTT, the primary genetic defect is known but the secondary consequences of that defect are poorly understood. Although key in beginning to understand disease processes, knowledge of the primary genetic defect alone often does not give insight into the mechanism of neuropathology, nor does it suggest obvious therapeutic strategies. Our results suggest that cDNA microarrays and other high throughput gene expression analyses (Colantuoni *et al.*, 2000), are useful in the identification of differentially expressed genes that are abnormally regulated as a consequence of a primary genetic defect. These regulated genes may be reflective of pathological mechanisms, and may reveal cellular pathways that have been perturbed in a disease state. Thus, cDNA microarray approaches will be useful in the investigation of the molecular pathology of human disease and the eventual identification of diagnostic and therapeutic targets. For many other brain disorders, such as autism and neuropsychiatric disorders, no primary genetic defects have been identified. Expression profiling techniques may be useful in the study of these disorders in order to identify biological substrates of neuropathogenesis independent of the discovery of primary genetic defects.

Conclusion

Microarrays and other methods of high-throughput gene expression analysis are changing the focus of research from findings relevant to the function of single genes, to findings encompassing thousands of genes and the complex interplay of intra- and intercellular transcriptional programs. The challenge now is to begin to bridge the gaps between genotype, gene expression changes, functional cell biology, and clinical phenotype.

ACKNOWLEDGMENTS

We thank the individuals and families who made donations to the brain banks, and the Brain and Tissue Bank for Developmental Disorders at the University of Maryland and the Harvard Brain and Tissue Bank for providing postmortem brains. We thank Incyte Genomics for providing microarray chips, and we thank Kirby Smith and N. Varg for helpful comments. Supported by grants from the International Rett Syndrome Association (to J.P.) and P01 HD24448 (to J.P., W.E.K., and S.N.).

REFERENCES

Ahlsen, G., Rosengren, L., Belfrage, M., Palm, A., Haglid, K., Hamberger, A., & Gillberg, C. (1993) Glial fibrillary acidic protein in the cerebrospinal fluid of children with autism and other neuropsychiatric disorders. *Biol. Psychiatry* **33,** 734–743.

Alizadeh, A., Eisen, M., Davis, R. E., Ma, C., Sabet, H., Tran, T., Powell, J. I., Yang, L., Marti, G. E., Moore, D. T., Hudson, J. R., Chan, W. C., Greiner, T., Weisenburger, D., Armitage, J. O., Lossos, I., Levy, R., Botstein, D., Brown, P. O., & Staudt, L. M. (1999) The lymphochip: A specialized cDNA microarray for the genomic-scale analysis of gene expression in normal and malignant lymphocytes. *Cold Spring Harb. Symp. Quant. Biol.* **64,** 71–78.

Allaman-Pillet, N., Djemai, A., Bonny, C., & Schorderet, D. F. (1998) Methylation status of CpG sites and methyl-CpG binding proteins are involved in the promoter regulation of the mouse Xist gene. *Gene Exp.* **7,** 61–73.

Amano, K., Nomura, Y., Segawa, M., & Yamakawa, K. (2000) Mutational analysis of the MECP2 gene in Japanese patients with Rett syndrome. *J. Hum. Genet.* **45,** 231–236.

Amir, R. E., & Zoghbi, H. Y. (2000) Rett syndrome: Methyl-CpG-binding protein 2 mutations and phenotype-genotype correlations. *Am. J. Med. Genet. (Semin. Med. Genet.)* **97,** 147–152.

Amir, R. E., Van den Veyver, I. B., Wan, M., Tran, C. Q., Francke, U., & Zoghbi, H. Y. (1999) Rett syndrome is caused by mutations in X-linked MECP2, encoding methyl-CpG-binding protein 2. *Nat. Genet.* **23,** 185–188.

Amir, R. E., Van den Veyver, I. B., Schultz, R., Malicki, D. M., Tran, C. Q., Dahle, E. J., Philippi, A., Timar, L., Percy, A. K., Motil, K. J., Lichtarge, O., Smith, E. O., Glaze, D. G., & Zoghbi, H. Y. (2000) Influence of mutation type and X chromosome inactivation on Rett syndrome phenotypes. *Ann. Neurol.* **47,** 670–679.

Armstrong, D. D. (1997) Review of Rett syndrome. *J. Neuropathol. Exp. Neurol.* **56,** 843–849.

Bauman, M. L., Kemper, T. L., & Arin, D. M. (1995a) Microscopic observations of the brain in Rett syndrome. *Neuropediatrics* **26,** 105–108.

Bauman, M. L., Kemper, T. L., & Arin, D. M. (1995b) Pervasive neuroanatomic abnormalities of the brain in three cases of Rett's syndrome. *Neurology* **45,** 1581–1586.

Belichenko, P. V., Hagberg, B., & Dahlstrom, A. (1997) Morphological study of neocortical areas in Rett syndrome. *Acta Neuropathol.* (Berlin) **93,** 50–61.

Belichenko, P. V., Oldfors, A., Hagberg, B., & Dahlstrom, A. (1994) Rett syndrome: 3-D confocal microscopy of cortical pyramidal dendrites and afferents. *Neuroreport* **5,** 1509–1513.

Bienvenu, T., Carrie, A., de Roux, N., Vinet, M. C., Jonveaux, P., Couvert, P., Villard, L., Arzimanoglou, A., Beldjord, C., Fontes, M., Tardieu, M., & Chelly, J. (2000) MECP2 mutations account for most cases of typical forms of Rett syndrome. *Hum. Mol. Genet.* **9,** 1377–1384.

Bittner, M., Meltzer, P., Chen, Y., Jiang, Y., Seftor, E., Hendrix, M., Radmacher, M., Simon, R., Yakhini, Z., Ben-Dor, A., Sampas, N., Dougherty, E., Wang, E., Marincola, F., Gooden, C., Lueders, J., Glatfelter, A., Pollock, P., Carpten, J., Gillanders, E., Leja, D., Dietrich, K., Beaudry, C., Berens, M., Alberts, D., & Sondak, V. (2000) Molecular classification of cutaneous malignant melanoma by gene expression profiling. *Nature* **406,** 536–540.

Bouton, C., & Pevsner, J. (2000) Dragon: database referencing of array genes online. *Bioinformatics* **16,** 1038–1039.

Broadie, K., Rushton, E., Skoulakis, E. M., & Davis, R. L. (1997) Leonardo, a Drosophila 14-3-3 protein involved in learning, regulates presynaptic function. *Neuron* **19,** 391–402.

Buyse, I. M., Fang, P., Hoon, K. T., Amir, R. E., Zoghbi, H. Y., & Roa, B. B. (2000) Diagnostic testing for rett syndrome by DHPLC and direct sequencing analysis of the MECP2 gene: Identification of several novel mutations and polymorphisms. *Am. J. Hum. Genet.* **67,** 1428–1436.

Cameron, E. E., Bachman, K. E., Myohanen, S., Herman, J. G., & Baylin, S. B. (1999) Synergy of demethylation and histone deacetylase inhibition in the re-expression of genes silenced in cancer. *Nat. Genet.* **21,** 103–107.

Cedar, H. (1988) DNA methylation and gene activity. *Cell* **53,** 3–4.

Cheadle, J. P., Gill, H., Fleming, N., Maynard, J., Kerr, A., Leonard, H., Krawczak, M., Cooper, D. N., Lynch, S., Thomas, N., Hughes, H., Hulten, M., Ravine, D., Sampson, J. R., & Clarke, A. (2000) Long-read sequence analysis of the MECP2 gene in Rett syndrome patients: Correlation of disease severity with mutation type and location. *Hum. Mol. Genet.* **9,** 1119–1129.

Chen, R. Z., Akbarian, S., Tudor, M., & Jaenisch, R. (2001) Deficiency of methyl-CpG binding protein-2 in CNS neurons results in a Rett-like phenotype in mice. *Nat. Genet.* **27,** 327–331.

Clayton-Smith, J., Watson, P., Ramsden, S., & Black, G. C. (2000) Somatic mutation in MECP2 as a non-fatal neurodevelopmental disorder in males. *Lancet* **356,** 830–832.

Colantuoni, C., Purcell, A. E., Bouton, C. M., & Pevsner, J. (2000) High throughput analysis of gene expression in the human brain. *J. Neurosci. Res.* **59,** 1–10.

Constancia, M., Pickard, B., Kelsey, G., & Reik, W. (1998) Imprinting mechanisms. *Genome Res.* **8,** 881–900.

Couvert, P., Bienvenu, T., Aquaviva, C., Poirier, K., Moraine, C., Gendrot, C., Verloes, A., Andres, C., Le Fevre, A. C., Souville, I., Steffann, J., des Portes, V., Ropers, H. H., Yntema, H. G., Fryns, J. P., Briault, S., Chelly, J., & Cherif, B. (2001) MECP2 is highly mutated in X-linked mental retardation. *Hum. Mol. Genet.* **10,** 941–946.

De Bona, C., Zappella, M., Hayek, G., Meloni, I., Vitelli, F., Bruttini, M., Cusano, R., Loffredo, P., Longo, I., & Renieri, A. (2000) Preserved speech variant is allelic of classic Rett syndrome. *Eur. J. Hum. Genet.* **8,** 325–330.

Deguchi, K., Antalffy, B. A., Twohill, L. J., Chakraborty, S., Glaze, D. G., & Armstrong, D. D. (2000) Substance P immunoreactivity in Rett syndrome. *Pediatr. Neurol.* **22,** 259–266.

DeRisi, J., Penland, L., Brown, P. O., Bittner, M. L., Meltzer, P. S., Ray, M., Chen, Y., Su, Y. A., & Trent, J. M. (1996) Use of a cDNA microarray to analyse gene expression patterns in human cancer. *Nat. Genet.* **14,** 457–460.

Dragich, J., Houwink-Manville, I., & Schanen, C. (2000) Rett syndrome: A surprising result of mutation in MECP2. *Hum. Mol. Genet.* **9,** 2365–2375.

Elek, J., Park, K. H., & Narayanan, R. (2000) Microarray-based expression profiling in prostate tumors. *In Vivo* **14,** 173–182.

Eng, L. F., Lee, Y. L., Kwan, H., Brenner, M., & Messing, A. (1998) Astrocytes cultured from transgenic mice carrying the added human glial fibrillary acidic protein gene contain Rosenthal fibers. *J. Neurosci. Res.* **53,** 353–360.

Goldman, J. E., & Corbin, E. (1991) Rosenthal fibers contain ubiquitinated alpha B-crystallin. *Am. J. Pathol.* **139,** 933–938.

Golub, T. R., Slonim, D. K., Tamayo, P., Huard, C., Gaasenbeek, M., Mesirov, J. P., Coller, H., Loh, M. L., Downing, J. R., Caligiuri, M. A., Bloomfield, C. D., & Lander, E. S. (1999) Molecular classification of cancer: class discovery and class prediction by gene expression monitoring. *Science* **286,** 531–537.

Guy, J., Hendrich, B., Holmes, M., Martin, J. E., & Bird, A. (2001) A mouse Mecp2-null mutation causes neurological symptoms that mimic Rett syndrome. *Nat. Genet.* **27,** 322–326.

Hagberg, B., Aicardi, J., Dias, K., & Ramos, O. (1983) A progressive syndrome of autism, dementia, ataxia, and loss of purposeful hand use in girls: Rett's Syndrome. Report of 35 cases. *Ann. Neurol.* **14,** 471–479.

Hakak, Y., Walker, J. R., Li, C., Wong, W. H., Davis, K. L., Buxbaum, J. D., Haroutunian, V., & Fienberg, A. A. (2001) Genome-wide expression analysis reveals dysregulation of myelination-related genes in chronic schizophrenia. *Proc. Natl. Acad. Sci.* USA **98,** 4746–4751.

Hampson, K., Woods, C. G., Latif, F., & Webb, T. (2000) Mutations in the MECP2 gene in a cohort of girls with Rett syndrome. *J. Med. Genet.* **37,** 610–612.

Hausser, A., Storz, P., Link, G., Stoll, H., Liu, Y. C., Altman, A., Pfizenmaier, K., & Johannes, F. J. (1999) Protein kinase C mu is negatively regulated by 14-3-3 signal transduction proteins. *J. Biol. Chem.* **274,** 9258–9264.

Head, M. W., Corbin, E., & Goldman, J. E. (1993) Overexpression and abnormal modification of the stress proteins alpha B-crystallin and HSP27 in Alexander disease. *Am. J. Pathol.* **143,** 1743–1753.

Horska, A., Naidu, S., Herskovits, E. H., Wang, P. Y., Kaufmann, W. E., & Barker, P. B. (2000) Quantitative 1H MR spectroscopic imaging in early Rett syndrome. *Neurology* **54,** 715–722.

Huppke, P., Laccone, F., Kramer, N., Engel, W., & Hanefeld, F. (2000) Rett syndrome: analysis of MECP2 and clinical characterization of 31 patients. *Hum. Mol. Genet.* **9,** 1369–1375.

Imessaoudene, B., Bonnefont, J. P., Royer, G., Cormier-Daire, V., Lyonnet, S., Lyon, G., Munnich, A., & Amiel, J. (2001) MECP2 mutation in non-fatal, non-progressive encephalopathy in a male. *J. Med. Genet.* **38,** 171–174.

Inui, M., Watanabe, T., & Sobue, K. (1994) Annexin VI binds to a synaptic vesicle protein, synapsin I. *J. Neurochem.* **63,** 1917–1923.

Iwaki, T., Kume-Iwaki, A., Liem, R. K., & Goldman, J. E. (1989) Alpha B-crystallin is expressed in non-lenticular tissues and accumulates in Alexander's disease brain. *Cell* **57,** 71–78.

Iwaki, T., Iwaki, A., Tateishi, J., Sakaki, Y., & Goldman, J. E. (1993) Alpha B-crystallin and 27-kd heat shock protein are regulated by stress conditions in the central nervous system and accumulate in Rosenthal fibers. *Am. J. Pathol.* **143,** 487–495.

Jackson, M., Gentleman, S., Lennox, G., Ward, L., Gray, T., Randall, K., Morrell, K., & Lowe, J. (1995) The cortical neuritic pathology of Huntington's disease. *Neuropathol. Appl. Neurobiol.* **21,** 18–26.

Jellinger, K., & Seitelberger, F. (1986) Neuropathology of Rett syndrome. *Am. J. Med. Genet. Suppl.* **1,** 259–288.

Jellinger, K., Armstrong, D., Zoghbi, H. Y., & Percy, A. K. (1988) Neuropathology of Rett syndrome. *Acta Neuropathol.* **76,** 142–158.

Jellinger, K. A. (2000) Cell death mechanisms in Parkinson's disease. *J. Neural. Transm.* **107,** 1–29.

Jones, D. H., Martin, H., Madrazo, J., Robinson, K. A., Nielsen, P., Roseboom, P. H., Patel, Y., Howell, S. A., & Aitken, A. (1995) Expression and structural analysis of 14-3-3 proteins. *J. Mol. Biol.* **245,** 375–384.

Kaufmann, W. E., Naidu, S., & Budden, S. (1995) Abnormal expression of microtubule-associated protein 2 (MAP-2) in neocortex in Rett syndrome. *Neuropediatrics* **26,** 109–113.

Kaufmann, W. E., Pearlson, G. D., & Naidu, S. (1998) The neuroanatomy of Rett syndrome: Neuromorphological and neuroimaging studies. *Rivista Medica* **4,** 187–199.

Kaufmann, W. E., Taylor, C. V., Hohmann, C. F., Sanwal, I. B., & Naidu, S. (1997) Abnormalities in neuronal maturation in Rett syndrome neocortex: Preliminary molecular correlates. *Eur. Child Adolesc. Psychiatry* **6**(Suppl. 1), 75–77.

Khan, J., Saal, L. H., Bittner, M. L., Chen, Y., Trent, J. M., & Meltzer, P. S. (1999) Expression profiling in cancer using cDNA microarrays. *Electrophoresis* **20,** 223–229.

Khan, J., Simon, R., Bittner, M., Chen, Y., Leighton, S. B., Pohida, T., Smith, P. D., Jiang, Y., Gooden, G. C., Trent, J. M., & Meltzer, P. S. (1998) Gene expression profiling of alveolar rhabdomyosarcoma with cDNA microarrays. *Cancer Res.* **58,** 5009–5013.

Kim, S. J., & Cook, E. H., Jr. (2000) Novel de novo nonsense mutation of MECP2 in a patient with Rett syndrome. *Hum. Mutat.* (Online) **15,** 382–383.

Laping, N. J., Teter, B., Nichols, N. R., Rozovsky, I., & Finch, C. E. (1994) Glial fibrillary acidic protein: Regulation by hormones, cytokines, and growth factors. *Brain Pathol.* **4,** 259–275.

Lekman, A. Y., Hagberg, B. A., & Svennerholm, L. T. (1991) Membrane cerebral lipids in Rett syndrome. *Pediatr. Neurol.* **7,** 186–190.

Lowe, J., Mayer, R. J., & Landon, M. (1993) Ubiquitin in neurodegenerative diseases. *Brain Pathol.* **3,** 55–65.

Lowe, J., McDermott, H., Pike, I., Spendlove, I., Landon, M., & Mayer, R. J. (1992a) alpha B crystallin expression in non-lenticular tissues and selective presence in ubiquitinated inclusion bodies in human disease. *J. Pathol.* **166,** 61–68.

Lowe, J., Errington, D. R., Lennox, G., Pike, I., Spendlove, I., Landon, M., & Mayer, R. J. (1992b) Ballooned neurons in several neurodegenerative diseases and stroke contain alpha B crystallin. *Neuropathol. Appl. Neurobiol.* **18,** 341–350.

Martin, H., Rostas, J., Patel, Y., & Aitken, A. (1994) Subcellular localisation of 14-3-3 isoforms in rat brain using specific antibodies. *J. Neurochem.* **63,** 2259–2265.

Meloni, I., Bruttini, M., Longo, I., Mari, F., Rizzolio, F., D'Adamo, P., Denvriendt, K., Fryns, J. P., Toniolo, D., & Renieri, A. (2000) A mutation in the rett syndrome gene, MECP2, causes X-linked mental retardation and progressive spasticity in males. *Am. J. Hum. Genet.* **67,** 982–985.

Messing, A., Head, M. W., Galles, K., Galbreath, E. J., Goldman, J. E., & Brenner, M. (1998) Fatal encephalopathy with astrocyte inclusions in GFAP transgenic mice. *Am. J. Pathol.* **152,** 391–398.

Mirnics, K., Middleton, F. A., Marquez, A., Lewis, D. A., & Levitt, P. (2000) Molecular characterization of schizophrenia viewed by microarray analysis of gene expression in prefrontal cortex. *Neuron* **28,** 53–67.

Mirnics, K., Middleton, F. A., Stanwood, G. D., Lewis, D. A., & Levitt, P. (2001) Disease-specific changes in regulator of G-protein signaling 4 (RGS4) expression in schizophrenia. *Mol. Psychiatry* **6,** 293–301.

Naidu, S. (1997) Rett syndrome: a disorder affecting early brain growth. *Ann. Neurol.* **42,** 3–10.

Nan, X., Campoy, F. J., & Bird, A. (1997) MeCP2 is a transcriptional repressor with abundant binding sites in genomic chromatin. *Cell* **88,** 471–481.

Nan, X., Cross, S., & Bird, A. (1998a) Gene silencing by methyl-CpG-binding proteins. *Novartis Found. Symp.* **214,** 6–16; Discussion 16–21, 46–50.

Nan, X., Ng, H. H., Johnson, C. A., Laherty, C. D., Turner, B. M., Eisenman, R. N., & Bird, A. (1998b) Transcriptional repression by the methyl-CpG-binding protein MeCP2 involves a histone deacetylase complex. *Nature* **393,** 386–389.

Ng, H. H., & Bird, A. (1999) DNA methylation and chromatin modification. *Curr. Opin. Genet. Dev.* **9,** 158–163.

Nielsen, J. B., Henriksen, K. F., Hansen, C., Silahtaroglu, A., Schwartz, M., & Tommerup, N. (2001) MECP2 mutations in Danish patients with Rett syndrome: High frequency of mutationss but no consistent correlations with clinical severity or with the X chromosome inactivation pattern. *Eur. J. Hum. Genet.* **9,** 178–184.

Norton, W. T., Aquino, D. A., Hozumi, I., Chiu, F. C., & Brosnan, C. F. (1992) Quantitative aspects of reactive gliosis: A review. *Neurochem. Res.* **17,** 877–885.

Obata, K., Matsuishi, T., Yamashita, Y., Fukuda, T., Kuwajima, K., Horiuchi, I., Nagamitsu, S., Iwanaga, R., Kimura, A., Omori, I., Endo, S., Mori, K., & Kondo, I. (2000) Mutation analysis of the methyl-CpG binding protein 2 gene (MECP2) in patients with Rett syndrome. *J. Med. Genet.* **37,** 608–610.

Oldfors, A., Hagberg, B., Nordgren, H., Sourander, P., & Witt-Engerstrom, I. (1988) Rett syndrome: Spinal cord neuropathology. *Pediatr. Neurol.* **4,** 172–174.

Oldfors, A., Sourander, P., Armstrong, D. L., Percy, A. K., Witt-Engerstrom, I., & Hagberg, B. A. (1990) Rett syndrome: Cerebellar pathology. *Pediatr. Neurol.* **6,** 310–314.

Orrico, A., Lam, C., Galli, L., Dotti, M. T., Hayek, G., Tong, S. F., Poon, P. M., Zappella, M., Federico, A., & Sorrentino, V. (2000) MECP2 mutation in male patients with non-specific X-linked mental retardation. *FEBS Lett.* **481,** 285–288.

Pegoraro, E., Schimke, R. N., Arahata, K., Hayashi, Y., Stern, H., Marks, H., Glasberg, M. R., Carroll, J. E., Taber, J. W., & Wessel, H. B., et al. (1994) Detection of new paternal dystrophin gene mutations in isolated cases of dystrophinopathy in females. *Am. J. Hum. Genet.* **54,** 989–1003.

Perou, C. M., Jeffrey, S. S., van de Rijn, M., Rees, C. A., Eisen, M. B., Ross, D. T., Pergamenschikov, A., Williams, C. F., Zhu, S. X., Lee, J. C., Lashkari, D., Shalon, D., Brown, P. O., & Botstein, D. (1999) Distinctive gene expression patterns in human mammary epithelial cells and breast cancers. *Proc. Natl. Acad. Sci.* USA **96,** 9212–9217.

Perou, C. M., Sorlie, T., Eisen, M. B., van de Rijn, M., Jeffrey, S. S., Rees, C. A., Pollack, J. R., Ross, D. T., Johnsen, H., Akslen, L. A., Fluge, O., Pergamenschikov, A., Williams, C., Zhu, S. X., Lonning, P. E., Borresen-Dale, A. L., Brown, P. O., & Botstein, D. (2000) Molecular portraits of human breast tumors. *Nature* **406,** 747–752.

Purcell, A. E., Jeon, O. H., Zimmerman, A. W., Blue, M. E., & Pevsner, J. Postmortem brain abnormalities of the glutamate neurotransmitter system in autism. *Neurology*, in press.

Razin, A. (1998) CpG methylation, chromatin structure and gene silencing-a three-way connection. *Embo. J.* **17,** 4905–4908.

Renkawek, K., Stege, G. J., & Bosman, G. J. (1999) Dementia, gliosis and expression of the small heat shock proteins hsp27 and alpha B-crystallin in Parkinson's disease. *Neuroreport* **10,** 2273–2276.

Renkawek, K., Voorter, C. E., Bosman, G. J., van Workum, F. P., & de Jong, W. W. (1994) Expression of alpha B-crystallin in Alzheimer's disease. *Acta Neuropathol.* (Berlin) **87,** 155–160.

Ross, D. T., Scherf, U., Eisen, M. B., Perou, C. M., Rees, C., Spellman, P., Iyer, V., Jeffrey, S. S., Van de Rijn, M., Waltham, M., Pergamenschikov, A., Lee, J. C., Lashkari, D., Shalon, D., Myers, T. G., Weinstein, J. N., Botstein, D., & Brown, P. O. (2000) Systematic variation in gene expression patterns in human cancer cell lines. *Nat. Genet.* **24,** 227–235.

Shahbazian, M. D., & Zoghbi, H. Y. (2001) Molecular genetics of Rett syndrome and clinical spectrum of MECP2 mutations. *Curr. Opin. Neurol.* **14,** 171–176.

Skoulakis, E. M., & Davis, R. L. (1998) 14-3-3 proteins in neuronal development and function. *Mol. Neurobiol.* **16,** 269–284.

Tomokane, N., Iwaki, T., Tateishi, J., Iwaki, A., & Goldman, J. E. (1991) Rosenthal fibers share epitopes with alpha B-crystallin, glial fibrillary acidic protein, and ubiquitin, but not with vimentin. Immunoelectron microscopy with colloidal gold. *Am. J. Pathol.* **138,** 875–885.

Vacca, M., Filippini, F., Budillon, A., Rossi, V., Mercadante, G., Manzati, E., Gualandi, F., Bigoni, S., Trabanelli, C., Pini, G., Calzolari, E., Ferlini, A., Meloni, I., Hayek, G., Zappella, M., Renieri, A., D'Urso, M., D'Esposito, M., MacDonald, F., Kerr, A., Dhanjal, S., & Hulten, M. (2001) Mutation analysis of the MECP2 gene in British and Italian Rett syndrome females. *J. Mol. Med.* **78,** 648–655.

Van den Veyver, I. B., & Zoghbi, H. Y. (2000) Methyl-CpG-binding protein 2 mutations in Rett syndrome. *Curr. Opin. Genet. Dev.* **10,** 275–279.

Van Der Hoeven, P. C., Van Der Wal, J. C., Ruurs, P., & Van Blitterswijk, W. J. (2000) Protein kinase C activation by acidic proteins including 14-3-3. *Biochem. J.* **347,** 781–785.

Wan, M., Lee, S. S., Zhang, X., Houwink-Manville, I., Song, H. R., Amir, R. E., Budden, S., Naidu, S., Pereira, J. L., Lo, I. F., Zoghbi, H. Y., Schanen, N. C., & Francke, U. (1999) Rett syndrome and beyond: Recurrent spontaneous and familial MECP2 mutations at CpG hotspots. *Am. J. Hum. Genet.* **65,** 1520–1529.

Wang, K., Gan, L., Jeffery, E., Gayle, M., Gown, A. M., Skelly, M., Nelson, P. S., Ng, W. V., Schummer, M., Hood, L., & Mulligan, J. (1999) Monitoring gene expression profile changes in ovarian carcinomas using cDNA microarray. *Gene* **229,** 101–108.

Watson, P., Black, G., Ramsden, S., Barrow, M., Super, M., Kerr, B., & Clayton-Smith, J. (2001) Angelman syndrome phenotype associated with mutations in MECP2, a gene encoding a methyl CpG binding protein. *J. Med. Genet.* **38,** 224–228.

Wu, V. W., & Schwartz, J. P. (1998) Cell culture models for reactive gliosis: New perspectives. *J. Neurosci. Res.* **51,** 675–681.

Xiang, F., Buervenich, S., Nicolao, P., Bailey, M. E., Zhang, Z., & Anvret, M. (2000) Mutation screening in Rett syndrome patients. *J. Med. Genet.* **37,** 250–255.

Xu, J., Stolk, J. A., Zhang, X., Silva, S. J., Houghton, R. L., Matsumura, M., Vedvick, T. S., Leslie, K. B., Badaro, R., & Reed, S. G. (2000) Identification of differentially expressed genes in human prostate cancer using subtraction and microarray. *Cancer Res.* **60,** 1677–1682.

Zhou, Y., Schopperle, W. M., Murrey, H., Jaramillo, A., Dagan, D., Griffith, L. C., & Levitan, I. B. (1999) A dynamically regulated 14-3-3, Slob, and Slowpoke potassium channel complex in Drosophila presynaptic nerve terminals. *Neuron* **22,** 809–818.